J. Materials, Conc. Struct. Pavements, JSCE, No. 718/V-57, 121-134, 2002 November

FLEXURAL FATIGUE FAILURE CHARACTERISTICS OF AN ENGINEERED CEMENTITIOUS COMPOSITE AND POLYMER CEMENT MORTARS

Peerapong SUTHIWARAPIRAK[1], Takashi MATSUMOTO[2] and Tetsushi KANDA[3]

[1]Member of JSCE, Graduate Student, Dept. of Civil Eng., The University of Tokyo
(Hongo 7-3-1, Bunkyo-ku, Tokyo 113-8656, Japan)
[2]Member of JSCE, Ph.D., Assistant Professor, Dept. of Civil Eng., The University of Tokyo
(Hongo 7-3-1, Bunkyo-ku, Tokyo 113-8656, Japan)
[3]Ph.D., Research Engineer, Kajima Technical Research Institute
(Tobitakyu 2-19-1, Chofu-shi, Tokyo 182-0036, Japan)

The fatigue failure characteristics of Engineered Cementitious Composite (ECC) were investigated by four-point flexural fatigue tests in comparison with two types of Polymer Cement Mortar (PCM). The fatigue failure mechanisms were observed, and the damage evolutions were measured for all shotcreted specimens. The results showed that ECC performs the improved fatigue life and that it exhibits a bilinear fatigue stress-life relation on a semi-logarithmic scale. ECC under fatigue loading shows much more ductility than PCMs, because the failure of ECC involves the initiation of multiple cracks, the propagation of those cracks, and the localization to a single crack, while the failure of PCMs involves only the initiation of a single crack.

Key Words: *ECC, fatigue life, fatigue failure mechanism, crack propagation, multiple cracks*

1. INTRODUCTION

The fatigue durability of a repair material is considered to be important in order to develop a feasible repair method for a structure subjected to fatigue loading. A cementitious composite shotcrete system is one of feasible repair methods for such a structure according to its simplicity in a construction process. It is increasingly introduced for several structural applications, such as a tunnel lining construction and a bridge deck repair construction. Although a cementitious matrix performs a tensile-weak behavior, discontinuous fibers can be mixed in the matrix in order to improve tensile and flexural properties of such a cementitious composite shotcrete system.

Engineered Cementitious Composite (ECC) and Polymer Cement Mortar (PCM) are examples of cementitious composites mixed with fibers for specific purposes. ECC is a cementitious composite developed following the concepts of fracture mechanics and micromechanics so that pseudo strain-hardening behavior can be obtained[1]. ECC performs very high strength and outstanding tensile strain capacity. For example, ECC that contains less than 2% volume fraction of polyethylene fibers can achieve 5% of the tensile strain capacity at failure. PCM is a cementitious structural repairing mortar, which consists of cement, liquid polymer, and polymeric fibers. PCM has low permeability, and it reduces the incidence of drying shrinkage cracking. According to the improved mechanical properties, PCM is increasingly applied to structural repair systems, and ECC will be introduced for structural applications in the near future.

Although there are many studies reporting the improvement in mechanical properties of ECC and PCM and the failure mechanisms of them under static loading conditions were presented[1), 2), 3)], there have been few studies related to their properties and failure mechanisms under a fatigue loading condition. The investigations on the fatigue properties and failure mechanisms are necessary for proposing a proper repair method and for developing high fatigue-resistant materials for structures subjected to fatigue loading.

The study on the fatigue failure mechanisms of materials is also important for the prospect of developing an analytical method for predicting the behaviors of structures subjected to fatigue loading. In the case of concrete and Fiber Reinforced Concrete (FRC), the propagation of a localized crack is considered as a dominant failure mechanism under flexural fatigue loading[4),5)], and it is successfully introduced as an assumption for predicting the flexural fatigue properties of those materials. For example, the finite element model that allows for the fatigue crack propagation as the failure mechanism has been developed for predicting the fatigue life of reinforced concrete and reinforced fiber concrete beams[6)]. It is demonstrated that based on the failure mechanism assumption of materials, the fatigue properties of cementitious composite structures can be predicted by mean of such a finite element analysis.

This study aims at investigating the fatigue properties as well as the fatigue failure mechanisms of ECC and PCMs. Four-point flexural fatigue test, a simple testing method in order to investigate fatigue properties of materials, was performed for a total number of 62 shotcreted specimens. Based on the fatigue failure mechanisms of materials, an analytical model is aimed to be developed in the further study for the prediction of fatigue properties of newly constructed structures as well as repaired structures.

2. TESTING PROGRAM

(1) Materials and shotcreted specimens

One specific type of ECC was investigated and compared with two types of PCM (here after referred to as PCMA and PCMB). PCMs used in this study are commercial cementitious structural repair mortars in a ready-to-use powder form. PCMA contains cement, fine aggregate, lightweight aggregate, and acrylic polymer fibers, while PCMB contains cement, fine aggregate, SBR polymer, and Poly Vinyl Alcohol (PVA) fibers. Both PCMs contain less than 0.5 % volume fraction of fibers, and the fibers in these PCMs do not induce the improvement of tensile properties of the cementitious matrix.

The ECC used in this study contains cement, fly ash, chemical admixtures, and Poly Vinyl Alcohol (PVA) fibers. PVA fibers of 0.04 mm in diameter and 12 mm in length are mixed by 2.1% volume fraction, V_f. The tensile strength of a single fiber is 1600 MPa. The mix proportion of the ECC is shown in **Table 1**.

Table 1 Mix proportion of ECC

W/B*	S/B**	Water kg/m^3	Fiber volume fraction, V_f(%)
0.32	0.42	382	2.1

* Water-cementitious material ratio

** Sand-cementitious material ratio

Shotcreted beam specimens of 100x100x400mm in dimensions were made. 20 specimens for each kind of PCMs and 22 specimens for the ECC were shotcreted in formworks. The shotcrete system is specified in details in Reference 7. After shotcreting, the specimens were cured under constant temperature of 20°C and humidity of 60 % for at least 2 months in order to alleviate the effect of initial curing time.

(2) Apparatus and test procedure

The apparatus employed in this study was a 200 kN capacity feed back controlled loading machine. For static loading, the tests were performed under a displacement control condition, while fatigue loading tests were performed under a load control condition.

Four-point flexural tests were conducted where specimens were simply supported on a clear span of 300 mm and subjected to two-point loads at one-third of the span.

Unnotced beam specimens were tested under both static and fatigue loading. The tests started after the two-month curing process by the order of PCMA, PCMB, and ECC. For each material, the flexural strength was determined by averaging the ultimate flexural strength of four specimens under static loading. Then, fatigue tests at different flexural fatigue stress levels were conducted.

a) Static test

Flexural static test was performed in accordance with JCI standard for test methods of FRC (JCI-SF4)[8)]. Monotonic increase of stroke at midspan was applied at the constant rate of 0.02 mm/sec.

b) Fatigue test

Flexural fatigue tests were performed under load control condition. Specimens were subjected to an 8 Hz sinusoidal cyclic loading. The ratio between the maximum flexural stress and the minimum flexural stress was set constantly equal to 0.2 for all specimens in order to avoid any impact and slip of specimens during testing.

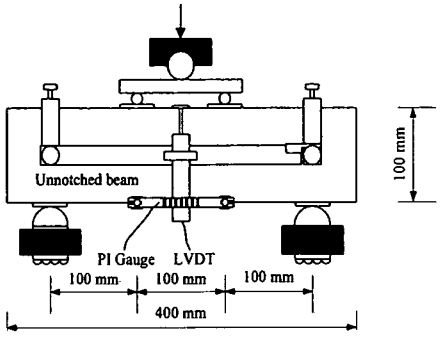

Fig.1 Experiment setting

At the first cycle, load was applied gradually to the maximum stress level in 50 seconds. The cyclic fatigue loading was, then, applied. The experiments were terminated either after the failure took place or the number of cycles was larger than two million.

In order to obtain the fatigue stress-life relation, specimens at four different fatigue stress levels were conducted. The flexural fatigue stress level, S, is defined as the ratio of the maximum fatigue stress to the average ultimate flexural strength. Four specimens were assigned for each fatigue stress level. The first stress level was the highest. The succeeding levels were smaller which were determined by considering the average fatigue life of the previous stress level.

(3) Data collection

Linear Variable Differential Transducers (LVDTs) were introduced to measure the deflection at the midspan of specimens. Two LVDTs were used to measure the midspan deflection change from both sides of specimens. They were mounted on a steel frame fixed on a specimen so that the displacement evolution produced only by the specimens can be measured. Two π gauges were used for measuring the displacement within ±50 mm span from the middle of specimens. They were attached to the lowest part of both sides of a specimen. Therefore, the measurement data from π gauges are representing the summation of the maximum crack width, which is equal to the Crack Mouth Opening Displacement (CMOD), of all cracks occurred in the measuring span and the elastic deformation of the specimen. Under fatigue loading, data at the maximum and the minimum stress level were recorded. The experimental setting was the same for both cases of the static test and the fatigue test as shown in **Fig.1**. In order to observe the initiation of cracks throughout the test, white paint was sprayed on both sides of specimens. The numbers of cycles at which cracks initiated and the number of cycles at which a specimen failed were recorded.

For ECC specimens, a microscope was additionally used in order to measure a Crack Mouth Opening Displacement (CMOD) of the localized crack that caused failure.

Table 2 Results of flexural static tests

Specimen	No.	Ultimate flexural load (kN) P_u	Ultimate flexural strength (MPa) σ_s	Average flexural strength (MPa) σ_a
PCMA	1	10.39	3.045	3.196
	2	11.33	3.251	
	3	11.33	3.292	
	4	10.78	3.167	
PCMB	1	18.57	5.444	5.335
	2	15.20	4.457	
	3	20.86	6.104	
	4	17.87	5.278	
ECC	1	27.68	8.151	8.709
	2	32.70	9.556	
	3	28.65	8.421	
	4	28.52	8.385	

3. STATIC TEST RESULTS

(1) Ultimate flexural load and strength

The ultimate flexural load, P_u, and the ultimate flexural strength, σ_s, of ECC specimens and PCM specimens under monotonic loading are summarized in **Table 2**. The ultimate flexural strength, σ_s, is calculated from the elastic beam formulation. It shows that ECC specimens exhibited much higher ultimate flexural strength than that of PCMs. The average ultimate flexural strength, σ_a, was used for determining the fatigue stress levels.

(2) Failure characteristics

The flexural stress-midspan deflection relationships of PCMA specimens are shown in **Fig.2(a)**. It is noted that the flexural stress here is not the stress at a local crack plane, but it is the applied flexural stress calculated from the elastic beam formulation. The relations between the flexural stress and the displacement measured by π gauges of PCMA specimens are shown in **Fig.2(b)**. The displacement measured by π gauges shown herein

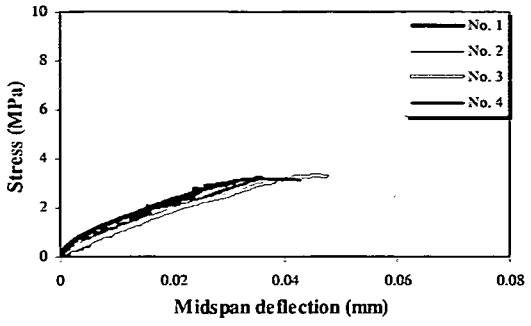

(a) Stress-midspan deflection relationships of PCMA specimens

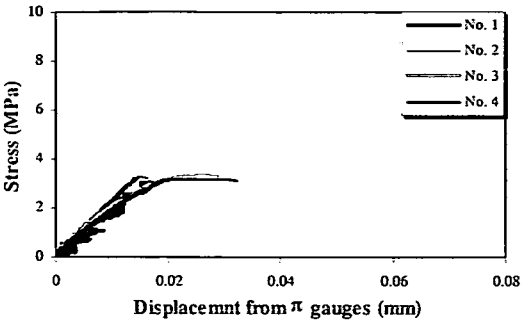

(b) Stress-displacement relationships of PCMA specimens

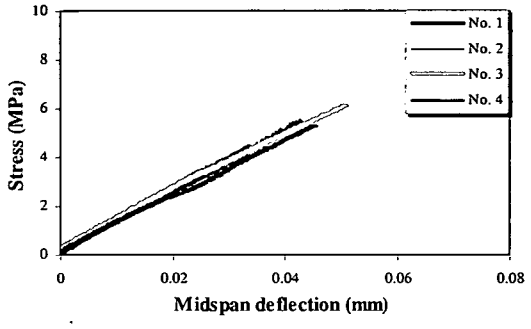

(c) Stress-midspan deflection relationships of PCMB specimens

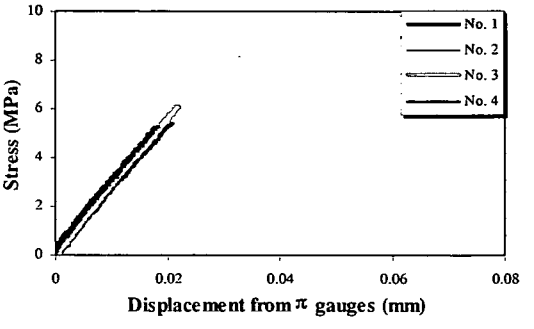

(d) Stress-displacement relationships of PCMB specimens

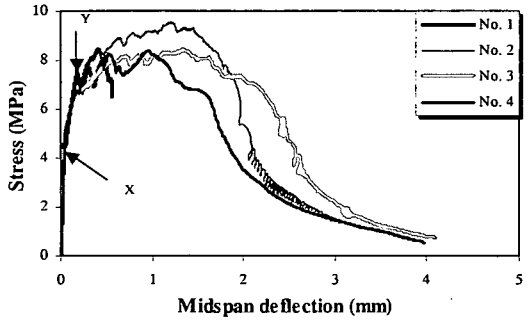

(e) Stress-midspan deflection relationships of ECC specimens

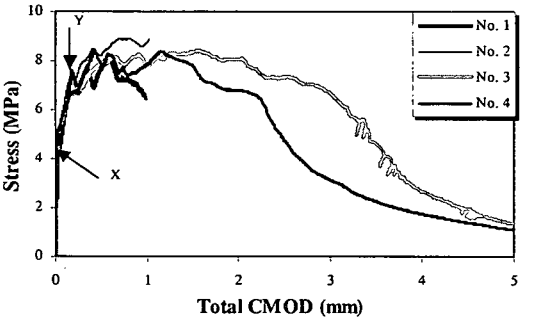

(f) Stress-total CMOD relationships of ECC specimens

Fig.2 Results of flexural static tests measured by LVDTs and π gauges

are the elastic elongation of specimens before cracking and the crack opening displacement of cracks initiated within the 100 mm length of the π gauges. The linear part of the curves indicated that no crack occurred within the early stage. For specimens 1 and 2, no crack was observed before the ultimate strength was attained with the sudden failure, while specimens 3 and 4 further sustained some tensile stress after the ultimate strength was reached. The midspan deflection increased significantly before the brittle failure took place. Since all specimens exhibited the sudden failure, the post-peak behavior of all PCMA specimens could not be detected by the measuring instruments.

The static test results of PCMB specimens are presented in **Fig.2(c) and 2(d)**. PCMB specimens showed more brittle failure than PCMA specimens. No nonlinear behavior was observed up to their sudden failure.

The ECC under monotonic loading demonstrated a very ductile behavior (**Fig.2(e) and 2(f)**). Initially, the specimens showed an elastic behavior. After microcracks initiated, its nonlinear behavior was observed upon the change of stiffness of curves (point X in figures). When the first visible crack initiated, the load dropped slightly (point Y in figures) before increasing again. New cracks, then, initiated consecutively and distributed along the tensile surface even in the shear span area. These distributed cracks opened with the increase of applied displacement. Finally, only one crack started to localize, and the load resistance dropped rapidly. The midspan deflection of specimens could be extended up to more than 4 mm.

The displacement measured by the π gauges in the 100 mm span presented in **Fig.2(f)** is the summation of the elastic elongation of matrix and the Crack Mouth Opening Displacement (CMOD) of multiple cracks in the measuring span. However, the elastic elongation of matrix is not substantially significant compared to the CMODs of cracks. Therefore, for ECC specimens, the displacement measured by the π gauges is approximately equal to the Total Crack Mouth Opening Displacement (TCMOD) of the cracks occurred within the measuring span.

The results clearly show that the ECC behaves in a more ductile manner than PCMs. The midspan deflection at ultimate strength of ECC specimens ranges from 1 to 2 mm, while that of PCM specimens ranges from 0.04 to 0.05 mm. According to the presence of multiple cracks, the hardening behavior of ECC provides very high tensile strain resistance.

The number of cracks was determined by a postmortem analysis. PCM specimens showed only 1 or 2 visible through-cracks, while ECC specimens showed about 10 visible through-cracks on the tension surface. This supports that the failure of PCMs involves a localized crack, while the failure of ECC involves the occurrence of multiple distributed cracks.

4. FATIGUE TEST RESULTS

The amount of specimens for each flexural fatigue stress level is shown in **Table 3**. 16 specimens of each kind of PCM (PCMA and PCMB) for four flexural stress levels and 18 specimens of ECC for five flexural stress levels were conducted.

Table 3 Number of specimens at each fatigue stress level

Materials	Level	1	2	3	4	5
PCMA	S *(%)	90	80	70	60	-
	Ns**	4	4	4	4	-
PCMB	S (%)	80	70	60	50	-
	Ns	4	4	4	4	-
ECC	S (%)	90	85	70	60	50
	Ns	4	4	4	4	2

*S = Fatigue flexural stress level
**Ns = Amount of specimens

(1) Failure characteristics

The fatigue progressive failure process and the initiation of cracks were observed and recorded for all specimens during fatigue loading. The illustration of midspan deflection evolution and the number of cycles in which cracks initiated are shown in **Fig.3** for each kind of materials subjected to 70% σ_a level.

a) Crack initiations

From the observation, no visible crack was observed in PCM specimens until just before their failure. PCMA specimens could resist some more cycles of loading after a crack initiated, while in the case of PCMB specimens, the initiation of a crack and the failure of a specimen took place nearly at the same time.

ECC specimens showed consecutive crack initiations, and, at the moment of each crack initiation, the increase of midspan deflection could be clearly observed. The moments in which crack initiated are marked on the graph by using dash lines (see **Fig.3(c)**).

b) Typical failure characteristics

It is noticed that the typical failure characteristics of these three materials can be divided into three phases as shown in **Fig.4**. Firstly, the damage of a specimen increases significantly at a small number of loading cycles. Secondly, the damage gradually increases with the increase of the number of cycles. Finally, the rapid increase in damage occurs due to the crack localization, followed by the failure of the specimen. The slope changes from mild slope in phase II to steep slope in phase III.

In a mechanical point of view, the failure characteristics of three materials are different from each other. The fatigue failure of two PCMs involves the initiation of a single crack while the fatigue failure of the ECC involves the initiation and the propagation of multiple cracks. These result ECC specimens to produce more damage evolution than PCM specimens. It can be noticed from the difference of phase II between PCM specimens and

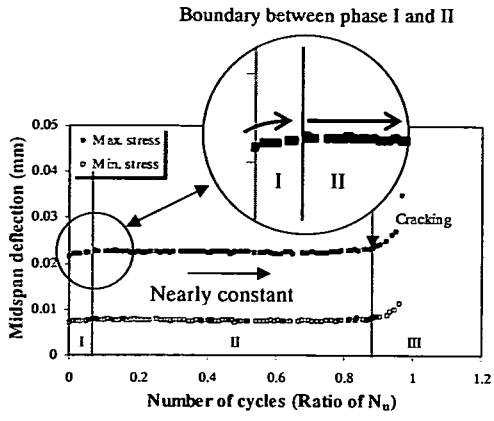

(a) PCMA specimen

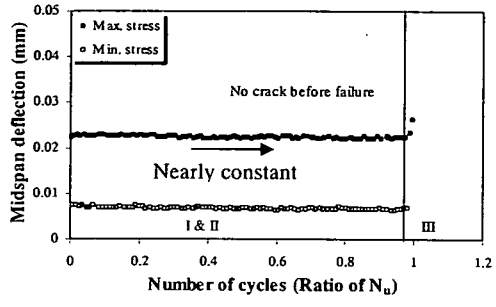

(b) PCMB specimen

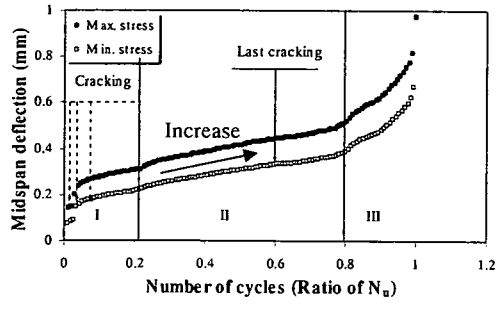

(c) ECC specimen

Fig.3 Initiation of cracks and evolution of midspan deflection for each kind of materials at 70% fatigue stress level

ECC specimens in **Fig.3**. PCM specimens showed nearly constant midspan deflection, while ECC specimens showed the large increase of midspan deflection in phase II.

PCM specimens under fatigue loading performed a very brittle failure behavior **(Fig.3(a) and 3(b))**. No visible crack was observed before the failure. The failure mechanism of PCMs presumably begins with

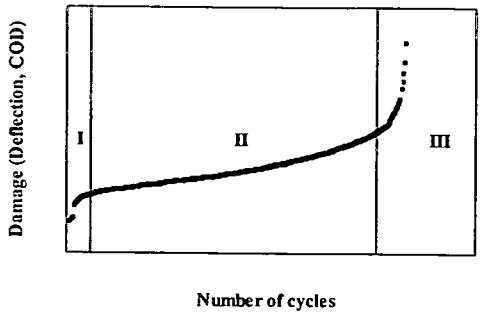

Fig. 4 Typical damage evolution of ECC and PCMs

the initiation of microcracks on the tension surface. The initiation of numerous microcracks at a small number of loading cycles results in the increase of damage in phase I. Because no macroscopic crack occurs in the initial period, the boundary between phase I and phase II is not obviously seen in the case of PCM specimens. The large circle in **Fig.3(a)** shows the enlarged illustration of the boundary between phase I and phase II. The increase of midspan deflection in phase I can be noticed before it becomes constant in phase II. Microcracks gradually initiate without the occurrence of a macroscopic crack. Therefore, the increase of damage is not significantly observed in phase II of **Fig.3(a) and 3(b)**. Finally, these microcracks convert to a localized crack. Since these PCMs contain only fine aggregates and small amounts of short discontinuous fibers, they cannot resist furthermore cycles of loading after the crack localization. This leads PCMs to break in a quite brittle manner as the rapid increase of slope in phase III before failure.

The fatigue failure of ECC specimens that showed a ductile behavior involves the initiation and propagation of distributed cracks. The three phases of failure evolution of the ECC are illustrated in **Fig.3(c)**. The fatigue failure process of the ECC can be explained as follows. At the first state of loading, a few visible cracks take place, and they produce the rapid increase in damage of a specimen (phase I). With further increase of fatigue loading cycles, energy dissipates both for the propagation of existing cracks and for the creation of new cracks. This process gradually develops so the gradual increase of damage is observed. This leads to the steady damage stage and results in the mild slope of damage evolution curve (phase II). Finally, only one crack tends to open significantly and it becomes the localized crack leading to the failure of the specimen. This can be shown by the rapid increase of damage again in phase III.

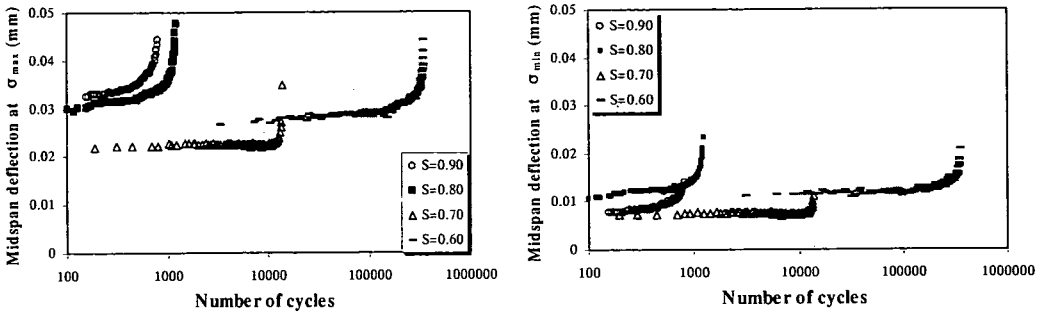

(a) PCMA specimens

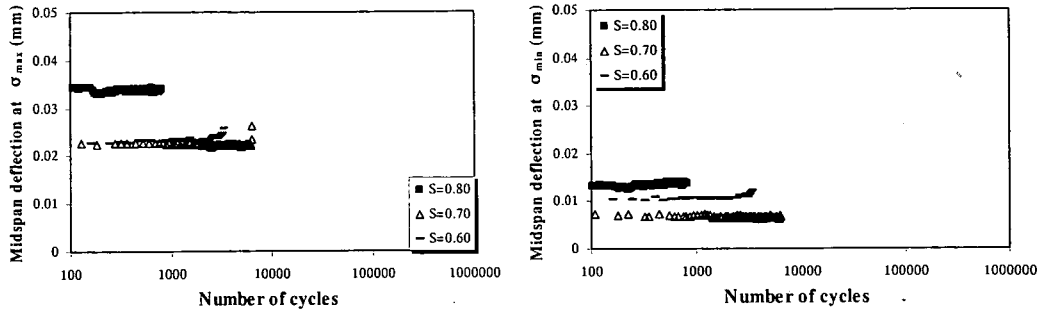

(b) PCMB specimens

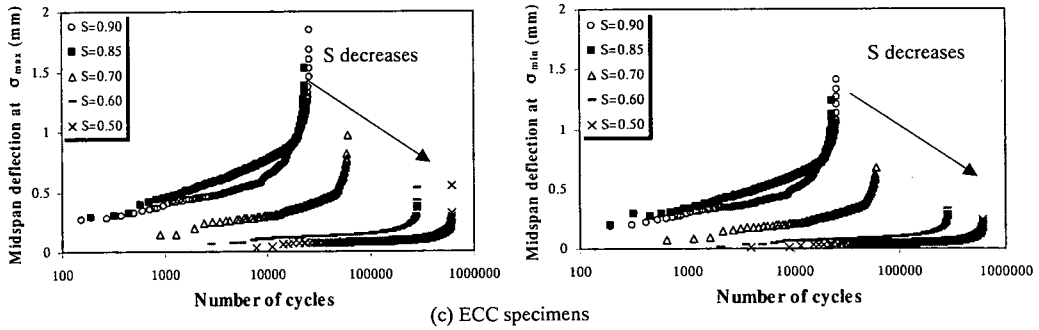

(c) ECC specimens

Fig.5 Evolution of midspan deflection under fatigue loading for each fatigue stress level, S, at the maximum stress, σ_{max}, and at the minimum stress, σ_{min}

(2) Damage characteristics of specimens

The midspan deflection and the displacement measured by π gauges are used as a damage index of specimens in this study. The evolutions of midspan deflection and π gauge measurement data with the increase of number of cycles are presented and discussed. The midspan deflection and crack measurement of all specimens were recorded at the maximum stress level and the minimum stress level. The number of cracks occurred under fatigue loading and the crack patterns in relation to the damage levels of specimens are discussed.

a) Deflection evolution

The evolutions of the average deflection from both sides of specimens were presented against the number of cycles, N, on a logarithmic scale in order to compare with other specimens of different fatigue stress levels, S. **Fig5(a), 5(b), and 5(c)** show the typical displacement evolution of specimens of each fatigue stress level of PCMA, PCMB, and ECC, respectively.

For PCM specimens, the evolution of midspan displacement up to the failure of specimens

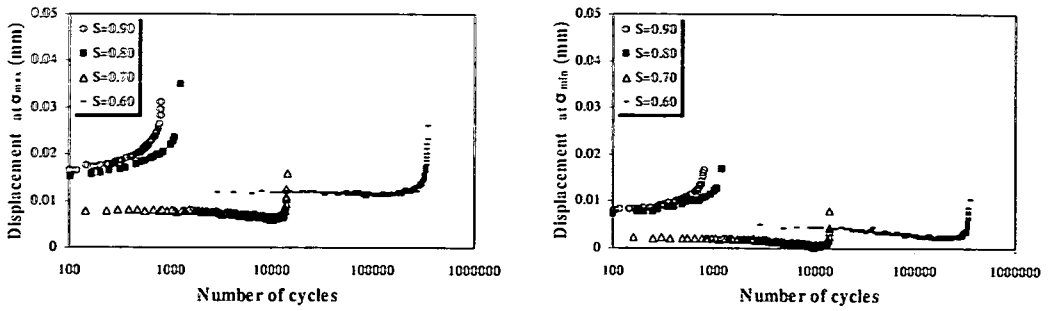

(a) PCMA specimens

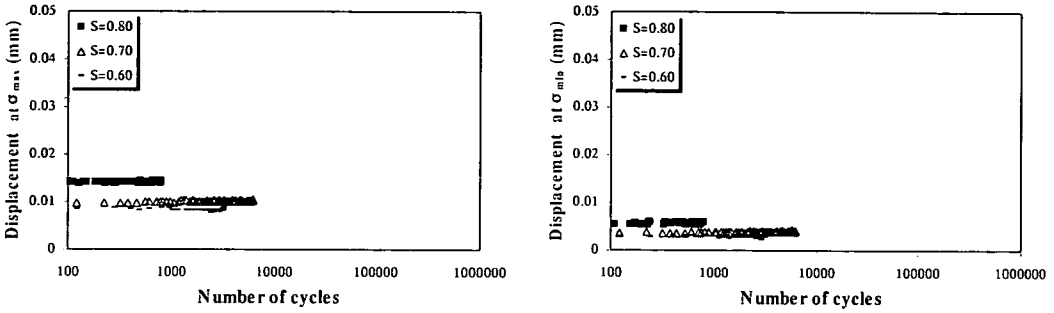

(b) PCMB specimens

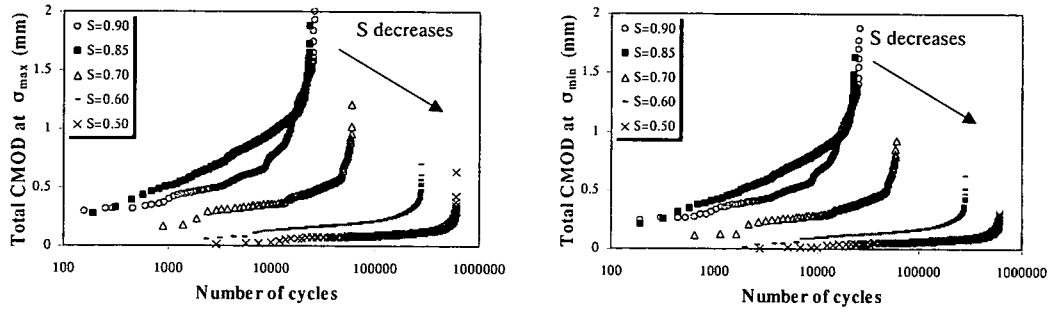

(c) ECC specimens

Fig.6 Evolution of displacement measured by π gauges under fatigue loading for each fatigue stress level, S, at the maximum stress, σ_{max}, and at the minimum stress, σ_{min}

increased in a small range, less than 0.05 mm. PCMA containing lightweight aggregates showed a more ductile behavior than PCMB. In the case of PCMB specimens, there was no substantial change in midspan deflection until their failure.

Similar to the static test results, ECC specimens performed a much more ductile behavior than those of PCMs under fatigue loading. The range of displacement evolution of ECC specimens at the maximum stress and minimum stress is much wider than those of PCM specimens, and it evolved up to about 2 mm midspan deflection before failure.

b) Crack measurement data

The displacement measured by π gauges in the 100 mm of measuring span is plotted against the number of cycles in **Fig.6**. Only typical result at each fatigue stress levels is shown in **Fig.6(a), 6(b), and 6(c)** for PCMA, PCMB, and ECC, respectively.

It is noticed that some PCM specimens, especially those with low fatigue stress levels, showed the decrease of displacement measured by π gauges with the increase of load cycles. This error might be caused by the misalignment of π gauges at the initial state.

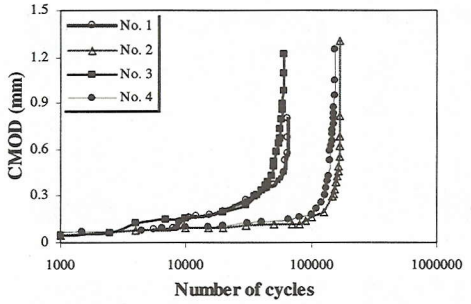

Fig.7 Evolution of CMOD of ECC specimens subjected to 70% σ_a measured by a microscope

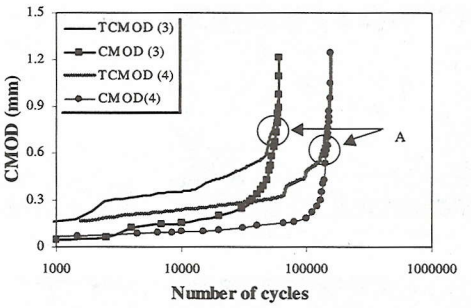

Fig.8 Evolution of CMOD of ECC specimens no. 3 and 4 in comparison with corresponding TCMOD

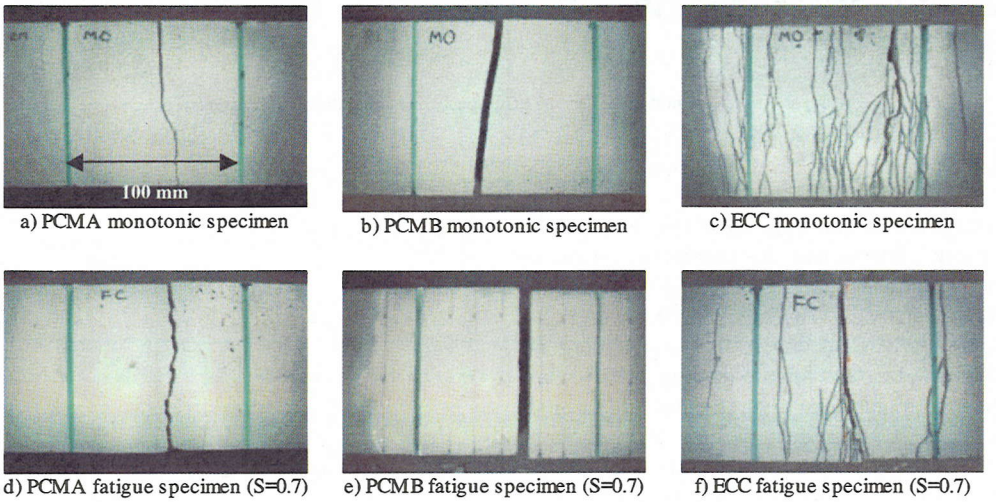

a) PCMA monotonic specimen b) PCMB monotonic specimen c) ECC monotonic specimen

d) PCMA fatigue specimen (S=0.7) e) PCMB fatigue specimen (S=0.7) f) ECC fatigue specimen (S=0.7)

Fig.9 Crack patterns on the bottom surface of monotonic and fatigue specimens of PCMA, PCMB and ECC

Crack Mouth Opening Displacement (CMOD) for the localized crack leading to the failure of ECC specimens measured by a microscope are plotted in **Fig.7**. The evolutions of CMOD of all four specimens at 70% fatigue stress level are selected for illustration. **Fig.8** presents the evolutions of CMOD of specimens 3 and 4 at 70% σ_a level comparing with their TCMOD. It was found that at low cycles, TCMOD, which is the summation of all distributed cracks, is much larger than CMOD of the localized crack. Then, both TCMOD and CMOD increase together, because the damage was distributed to all cracks. Finally, a crack localizes and its CMOD increases rapidly until it equals to TCMOD (Point A in **Fig.8**). This means only the localized crack opens, while other cracks close before failure.

c) Damage level

The midspan deflection and the displacement measured by π gauges are considered as an index for indicating the damage level of specimens. From the results of the evolutions of midspan deflection and crack measurement data shown earlier, it is noticed that the difference in the fatigue stress level applied to PCM specimens did not cause a significant difference in the damage level. This is because the fatigue failure of PCMs involves single crack failure as mentioned in the previous section.

By contrast, the damage level of ECC specimens depends on the fatigue stress level, S. The specimens were highly damaged at a high stress level, and the level of damage decreased with the decrease of fatigue stress level, S. This is caused by the fact that ECC specimens exhibited multiple distributed cracks before failure and that the number of cracks initiated is larger when the specimens underwent high fatigue stress levels. The relationship between the number of

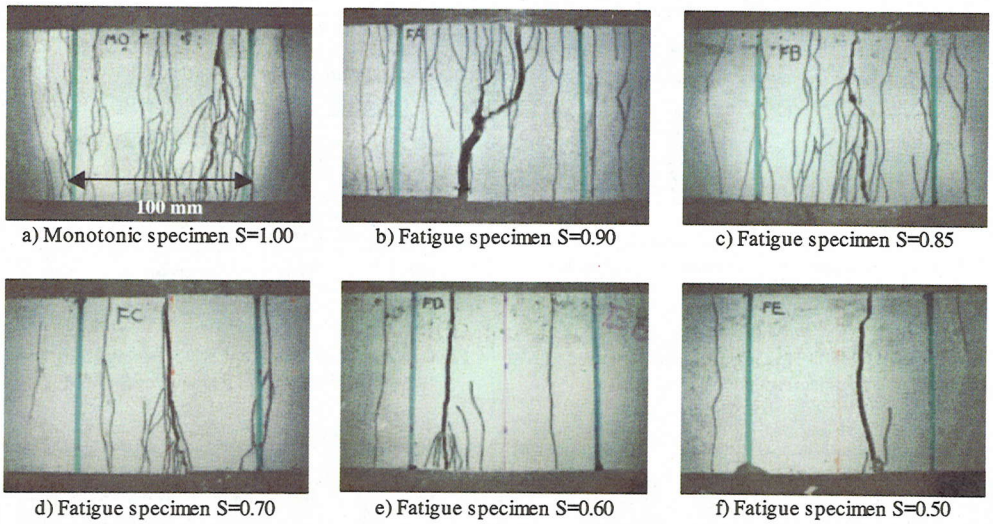

a) Monotonic specimen S=1.00 b) Fatigue specimen S=0.90 c) Fatigue specimen S=0.85

d) Fatigue specimen S=0.70 e) Fatigue specimen S=0.60 f) Fatigue specimen S=0.50

Fig. 10 Crack patterns on the bottom surface of ECC specimens under different fatigue stress levels

cracks and fatigue stress level is discussed in details later.

d) Crack patterns and number of cracks

The crack patterns and the number of cracks of broken specimens were investigated by a postmortem analysis. The crack patterns of PCM specimens and ECC specimens that have undergone monotonic loading and fatigue loading (S=0.70) are illustrated in **Fig.9**. The figures show all through cracks in the 100-mm flexural span of the bottom surface after the failure of the specimens. It is obvious that ECC specimens exhibited different crack patterns from those of PCM specimens. Both PCMA and PCMB specimens showed single cracking failure (**Fig.9(a), 9(b), 9(d), and 9(e)**), while ECC specimens performed multiple cracking failure (**Fig.9(c) and 9(f)**). These strongly support the reason why ECC specimens produced more damage evolution, such as the increase of midspan deflection and CMOD, than PCM specimens.

According to the brittle failure characteristic of PCMs, both PCMA and PCMB under fatigue loading produced only a few cracks. Both monotonic and fatigue specimens showed only one through crack. The crack patterns of PCM specimens under fatigue loading are similar to those of specimens under static loading. Furthermore, there is no substantial difference in crack patterns as well as the number of through cracks at different fatigue stress levels.

The distributed cracks on the bottom surface of ECC specimens after their failure are illustrated in **Fig.10**. The crack patterns of fractured specimens

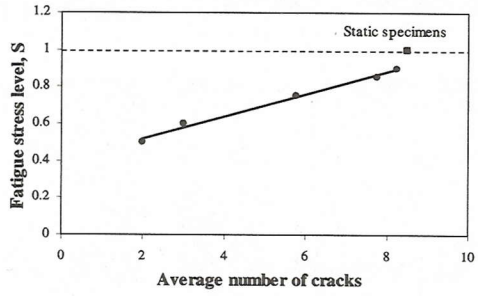

Fig.11 Relation between average number of cracks among four specimens and fatigue stress level of ECC

subjected to the different fatigue stress levels are shown in comparison with the crack pattern of a specimen that has undergone static loading. In fact, there are numerous discontinuous cracks initiated under both loading condition, however, only through cracks are illustrated in the figure. The results conclusively show that the number of cracks and the damage level of ECC specimens decrease with the decrease of fatigue stress level.

The relation between the fatigue stress level and the average numbers of cracks after failure is plotted in **Fig.11**. It can be observed that the number of cracks occurred in the specimens under high fatigue stress levels is higher than those of low fatigue stress levels. This conforms to the results of midspan deflection and crack measurement data evolution. It can be concluded that the level of damage evolution

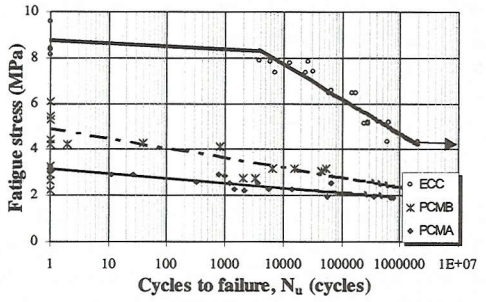

Fig.12 Fatigue stress-life relationships

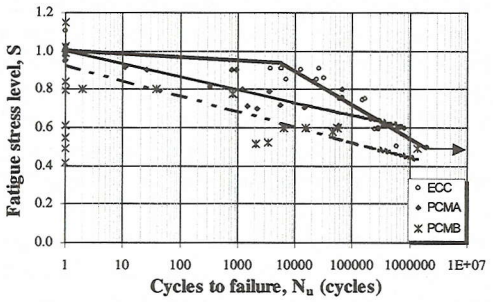

Fig.13 Fatigue stress level-life relationships

is governed by the number of distributed cracks initiated. Moreover, it is concluded that the number of cracks and the damage level of flexural static tested specimens is the highest and that they decrease with the decrease in fatigue stress level.

(3) Fatigue life

The flexural fatigue stress-life (the cycles to failure, N_u) relations of all three materials are plotted on a semi-logarithmic scale as shown in **Fig.12**. The arrow indicates the specimen that reached two million cycles without failure. It is obviously seen that at the same fatigue stress, the fatigue life of ECC is much longer than those of PCMs according to the much higher ultimate flexural strength of ECC.

The relations between the fatigue stress level, S, and the cycles to failure, N_u, (S-N relation) of all materials plotted on a semi-logarithmic scale are shown in **Fig.13**. It is noticed that under high fatigue stress levels, the ECC performs much longer fatigue life than those of PCMs. However, at lower fatigue stress levels, all materials tend to provide nearly the same fatigue life.

It is found that the ECC showed the bilinear relation on a semi-logarithmic scale, while PCMs showed the linear relation on a semi-logarithmic scale. From **Fig.13**, the flexural fatigue stress level-life relations of three materials can be

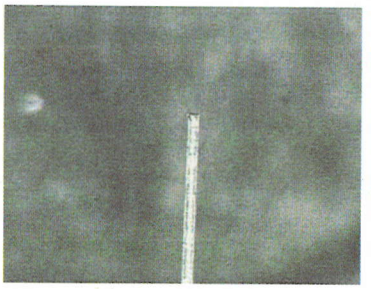

a) Fiber in virgin state

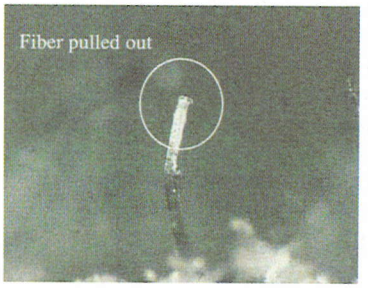

b) Fibers on the crack plane of a static specimen

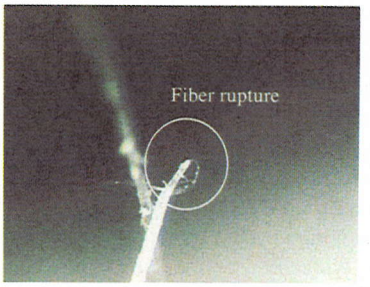

c) Fibers on the crack plane of a fatigue specimen

Fig.14 Microscopic images of 40μm PVA fibers

expressed by the relation between the fatigue stress level, S, and a logarithmic function of the number of cycles to failure, N_u, and they are given by:

PCMA:

$S = 1.001-0.0670\text{Log}(N_u)$ $\quad 1 \le N_u \le 2\text{x}10^6$;

PCMB:

$S = 0.928-0.0808\text{Log}(N_u)$ $\quad 1 \le N_u \le 2\text{x}10^6$;

ECC:

$S = 1.000-0.0226\text{Log}(N_u)$ $\quad 1 \le N_u < 1\text{x}10^4$

$S = 1.595-0.1750\text{Log}(N_u)$ $\quad 1\text{x}10^4 \le N_u \le 2\text{x}10^6$;

where S refers to the fatigue stress level or the ratio of the maximum flexural fatigue stress, σ_{max}, to the

average ultimate flexural strength, σ_a.

It can be noticed that fatigue stress-life relation of the ECC is similar to that of metallic materials, that is, it shows a bilinear relation on a semi-logarithmic scale. The S-N relation of ECC at the small number of cycles ($N \leq 10^4$) is obtained from the data of the monotonic specimens (S=1.0) and the fatigue specimens at S=0.9. Although there is no data between S=0.9 to S=1.0, the fatigue life might be expected to scatter around the line connected between S=1 and S=0.9.

The difference of S-N relation of the ECC from those of PCMs might be explained by the consideration of fiber rupture on the crack plane of ECC specimens. **Fig.14** shows the microscopic image of a 40μm PVA fiber a) in virgin state, b) on the crack plane of a monotonic specimen, and c) on the crack plane of a fatigue specimen, respectively. It is found from the observation that there are both fibers that were pulled out and fibers that were broken on the crack planes, and it is also noticed that amount of fibers that were broken on the crack plane of the monotonic specimen is less than that of the fatigue specimen. Most of fibers tended to be broken in the specimens subjected to fatigue loading. Therefore, it can be deduced that the fiber rupture might govern the fatigue life of this type of ECC.

This implies that the fatigue life of this ECC is in turn governed by that of bridging fiber. Usually, the fatigue life of material is expressed with a bilinear S-N diagram on a logarithmic scale. Such a bilinear diagram is composed of two power law equations for low cycle and high cycle fatigue region respectively, and it is typically seen in metallic materials. Although ECC and fibers inside are non-metallic materials, it exhibits a metallic-like bilinear S-N relation because the fatigue rupture failure of fibers, which governs the ECC failure, is similar to the fatigue rupture of metallic materials.

The study of effect of fiber fatigue rupture on fatigue failure is, therefore, necessary for the development of an ECC for high fatigue resistance.

5. DISCUSSION ON FAILURE MECHANISMS

The progressive fatigue damage in cementitious materials, such as concrete and mortar, involves the dominant crack initiation period and the crack propagation period. In order to develop a model for predicting fatigue life of cementitious materials, the failure mechanisms should be considered as the basis of the analytical model. In the case of FRC, the fatigue failure begins with the initiation of a single crack. This crack propagates further due to the degradation of transferred stress across the crack under fatigue loading. Then, the crack becomes a localized crack so that the damage increases rapidly before failure.

In order to develop an analytical model for predicting fatigue properties of FRC structural members, the fatigue propagation of the localized crack was investigated. It was considered as the dominant mechanism influencing the flexural fatigue failure of structural members[4), 5), 6)].

In the cases of the PCMs and the ECC, although they are cementitious composites, they behave in a different manner from FRC. The sudden failure of the PCMs and the pseudostrain hardening of the ECC cause the differences in fatigue failure mechanisms from FRC. The fatigue failure of PCMs involves primarily the initiation of cracks, as sudden failure takes place just after cracking. By contrast, the ECC with pseudostrain hardening behavior performs several distributed cracks under flexural fatigue loading and the number of cracks or the size of fracture zone depends on fatigue stress level as discussed earlier. The fatigue life of the ECC also involves the time for initiation of distributed cracks in matrix. The failure mechanisms of the materials under flexural fatigue loading are discussed below for the further analytical model development.

(1) Fatigue failure of the PCMs

The PCM specimens under flexural fatigue loading performed very brittle failure. The fatigue failure of the PCMs is governed by the initiation of a single crack. Failure takes place suddenly just after the first crack initiates. Therefore, the total fatigue life of the PCMs is almost identical to the number of load cycles from first loading to the cycles at which the first crack initiates.

In order to simulate the fatigue failure of the PCMs, the localized crack initiation process should be considered as a primary mechanism. Under progressive fatigue loading, microcracks gradually transfer to a localized crack. The reduction of cracking stress or cracking strain under fatigue loading might be an essential process that governs the fatigue life. The further investigation on the mechanism of fatigue crack initiation is necessary for the development of the analytical model.

(2) Fatigue failure of the ECC

As mentioned earlier, the fatigue stress level-life relation of the ECC can be represented by a bilinear logarithmic function. The extended fatigue life of the

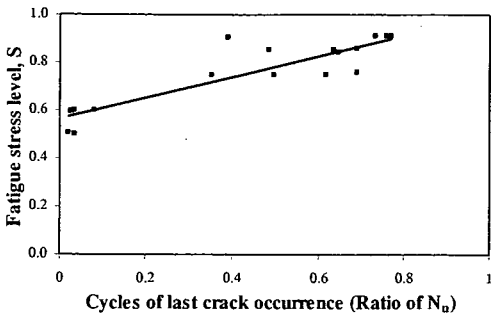

Fig.15 Relation between number of cycles that the last through crack occurred and fatigue stress level of ECC specimens

ECC at high stress levels results from the occurrence of multiple cracks. **Fig.15** shows the number of cycles to the occurrence of the last through crack normalized by the number of cycles to failure corresponding to the fatigue stress level. It can be noticed that the ratio of number of cycles decreases with the decrease of fatigue stress level.

At high fatigue stress level, several distributed cracks took place. The distributed cracks encouraged the distribution of damage and opposed the formation of a localized crack. Instead of motivating the crack localization, applied energy due to fatigue loading was distributed to all the cracks. At low fatigue stress level, the initiation of cracks spent very small number of cycles. The localization of a crack happens relatively early. As a result, there was no additional prolonged life for the ECC specimens under low fatigue stress level.

The flexural fatigue failure of the ECC depends on both the initiation of cracks and the propagation of cracks. The total fatigue life of the ECC expressed in the number of load cycles is the summation of the number of cycles for the initiation of distributed cracks, for gradual damage distribution on those cracks, and for the propagation of a localized crack towards the failure.

In order to reproduce the fatigue failure of the ECC by an analytical model, the effect of distributed cracks and their stress degradation interaction should be taken into account. The consequent crack initiations and propagations should be considered as major mechanisms in the analytical model.

The material model under fatigue loading or the stress degradation relation of ECC is developed for fatigue analysis based on the consideration of the stress degradation caused by fiber fatigue and interfacial bond fatigue[9]. In order to develop an analytical model for structural application, FEM is considered as an one of the effective methods. In the model development, the effect of multiple cracks and crack propagation mechanisms should be considered. Smeared crack elements for representing multiple cracking process and discrete crack elements for representing localized cracking process are introduced in the FEM model. For example, in the case of flexural beams, the degradation of the transferred stress in smeared crack elements under fatigue loading leads to the initiation of new multiple cracks. This is represented by the expansion of a fracture zone of smeared crack elements in the tension side with the increase of number of loading cycles. The degradation of transferred stress across crack in the discrete crack elements causes the propagation of a localized cracks that leads to the final failure of a fatigue beam.

6. CONCLUSIONS

The failure mechanisms and properties of PCMs and an ECC with PVA fibers have been investigated by the four-point flexural tests.

Under static loading, the PCMs performed very brittle behavior. Sudden failure took place just after first cracking. For the ECC, it showed a much more ductile behavior due to its pseudostrain hardening behavior. Distributed cracks occurred consecutively, so that it produced very high midspan deflection of more than 1 or 2 mm at the ultimate flexural strength.

The ECC specimens tested for flexural fatigue also performed a much more ductile behavior than the PCMs. The failure mechanism of the PCMs is governed by the initiation of a localized crack. The PCMs cannot resist tensile stress after cracking, and sudden failure takes place. The total fatigue life of PCM is nearly identical to the number of cycles to the first cracking. By contrast, the flexural fatigue failure of the ECC involves both the initiation of cracks and the propagation of cracks. The total fatigue life of the ECC stems from the summation of the number of cycles for the initiation of distributed cracks, for the gradual damage distribution onto those cracks, and for the propagation of a localized crack towards failure.

The effects of the initiation of distributed cracks and the interaction among those cracks on the fatigue life of the ECC are demonstrated in this study. It is shown that the damage and the number of cracks occurred in the specimens subjected to high fatigue stress level were larger than those subjected to lower one. The effect of the pseudostrain hardening prolongs the flexural fatigue life of the ECC.

For the fatigue life, at high fatigue stress level, the

ECC performed much longer life than the PCMs, while it tended to be equal to the fatigue life of PCMs at low fatigue stress level. The S-N relation of the ECC exhibits a bilinear function on a semi-logarithmic scale, which is similar to the S-N relation of a metallic material. From the observation of the failure crack plane of specimens, it is found that fibers in specimens under fatigue loading tend to be broken. The fiber rupture might govern the fatigue life of ECC. Moreover, the failure characteristic of fibers is similar to those of metallic materials that show rupture failure under fatigue loading. This might be the reason why ECC shows a bilinear S-N relation.

The failure mechanisms and failure characteristics of the ECC and the PCMs are discussed for the further analytical model development. In order to predict the fatigue properties and characteristics of the materials in structural applications, analytical models based on assumptions adopted from the failure mechanisms of materials is considered as the further study.

ACKNOWLEDGEMENT: The authors would like to express their gratitude towards the Kajima Technical Research Institute for producing all specimens and for valuable discussions to accomplish this study.

REFERENCES

1) Li, V. C.: From Micromechanics to Structural Engineering-The Design of Cementitious Composites for Civil Engineering Application, *Journal of Structural Mechanics and Earthquake Engineering*, Vol. 10, No. 2, pp. 37-48, 1993.
2) Kanda, T. and Li, V.C.: New Micromechanics Design Theory for Pseudostrain Hardening Cementitious Composite, *Journal of Engineering Mechanics*, Vol. 125, No. 4, pp. 373-381, 1999.
3) Ohama, Y. : Recent Progress in Concrete-Polymer Composites, *Advanced Cement Based Materials*, Vol. 5, No. 2, pp. 31-40, 1997.
4) Zhang, J.: Fatigue Fracture and Fiber Reinforced Concrete-An experimental and Theoretical Study, Doctoral Thesis, Technical University of Denmark, 1998.
5) Matsumoto, T., and Li, V. C.: Fatigue Life Analysis of Fiber Reinforced Concrete with a Fracture Mechanics Based Model, *Journal of Cement and Concrete Composites*, Vol. 21, No. 4, pp. 249-261, 1999.
6) Suthiwarapirak, P., Matsumoto, T. and Horii, H.: Fatigue Life Analysis of Reinforced Steel-Fiber-Concrete Beams, *Proceedings of the Japan Concrete Institute*, Vol. 23, No. 3, pp. 127-132, 2001.
7) Kanda, T., Saito, T., Sakata, N., and Hiraishi, M.: Fundamental Properties of Directed Sprayed Retrofit Material Utilizing Fiber Reinforced Pseudo Strain Hardening Cementitious Composites, *Proceedings of the Japan Concrete Institute*, Vol. 23, No. 1, pp. 475-480, 2001.
8) Japan Concrete Institute: *JCI Standards for Test Methods of Fiber Reinforced Concrete*, pp. 45-48, 1984.
9) Matsumoto, T, Suthiwarapirak, P., and Asamoto, S.: Model Development of ECC Fatigue Analysis, *Proceedings of the Japan Concrete Institute*, Vol. 24, No. 1, pp. 237-242, 2002 (In Japanese).

(Received December 27, 2001)

ECC とポリマーセメントモルタルの曲げ疲労破壊特性

スティワラピラク　ピーラポン・ 松本　高志・ 閑田　徹志

ECC の疲労破壊特性の把握を目的として四点曲げ疲労載荷による実験を行い，ポリマーセメントモルタル（PCM）との比較を行った．供試体は吹付けにより作成され，疲労破壊機構の把握と損傷進展・疲労寿命の計測を行った．その結果，ECC は優れた疲労寿命を示し，片対数上の S-N 曲線は金属の疲労破壊挙動に似た二直線型のものとなった．ECC の優れた疲労変形挙動は特異な破壊機構によるものであり，ECC の破壊機構は，複数ひび割れの発生と進展の後，局所化ひび割れの進展に支配されるのに対し，PCM は最初のひび割れの発生に主に支配されることが明らかとなった．